

**DEVELOPMENT OF NANOCOMPOSITE NANOWIRES BY
ELECTROSPINNING AS A SUPERCAPACITOR
ELECTRODE WITH HIGH ENERGY DENSITY, POWER
DENSITY AND RATE CAPABILITY**

VIDYADHARAN BAIJU

**Thesis submitted in fulfilment of the requirements for the award of
degree of Doctor of Philosophy in Advanced Materials**

**Faculty of Industrial Sciences & Technology
UNIVERSITI MALAYSIA PAHANG**

JANUARY 2015

ABSTRACT

Deployment of renewable energy requires, in addition to efficient energy conversion devices, electrochemical materials capable of storing a large amount of electrical energy as well as delivering it at a high rate. Electrochemical capacitors represent a class of energy storage devices; thus optimizing the working electrodes for them is the key to achieving high energy (E_S) and power densities (P_S). However, E_S and P_S are not united in the existing devices. High electrochemical reversibility, multiple oxidation states, high surface area and high electrical conductivity are requirements for high E_S and P_S in supercapacitor electrodes. Most materials offering high theoretical capacitance owing to its multiple oxidation states have lesser electrical conductivity; therefore, it is hypothesized that the electrical conductivity plays a dominant role in combining E_S and P_S in a single device. One-dimensional (1D) nanowires show improved charge transport properties compared to their nanoparticle analogue; therefore, they are expected to deliver simultaneously E_S and P_S in a single device. Studies show that the ceramic electrode materials exhibits diverse range of capacitances and conductivities than other choice of materials; therefore, the target device could be achieved using ceramic electrodes. Three typical materials with nanowire morphology are chosen for this purpose, viz. copper oxide (CuO), nickel oxide (NiO), and cobalt oxide (Co₃O₄). Among them NiO and Co₃O₄ show larger theoretical capacitance estimated at 2570 and 3560 Fg⁻¹ respectively, compared to CuO (1800 Fg⁻¹); the later has larger electrical conductivity. Synthesizing a composite is one of the methods to combine the functions of different materials; therefore, CuO+NiO and CuO+Co₃O₄ composites are the target materials. These materials were synthesized as 1D nanowires using an aqueous polymeric solution based electrospinning process and their structural properties by X-ray and electron diffraction were studied, high resolution transmission electron microscopy; morphological properties by scanning and transmission electron microscopy; and electrochemical properties by cyclic voltammetry, galvanostatic charge discharge cycling, and electrochemical impedance spectroscopy. The electrochemical studies showed that CuO, NiO and Co₃O₄ achieve a specific capacitance (C_S) nearly 30% of its theoretical value, but with low rate capability. The studies showed higher rate capability, lower equivalent series and charge transfer resistances in NiO + CuO and Co₃O₄+CuO composites than those of their single components. Asymmetric supercapacitor (ASC) using ceramic nanowire anode and commercially available activated carbon cathode were fabricated and their charge storage performance was compared with a symmetric supercapacitor fabricated using activated carbon at both electrodes. The ASC showed seven times higher specific capacitance and E_S compared to the symmetric device. The P_S decreased with E_S for devices employed single component ceramic nanowires. However, E_S remained practically same for increased P_S when their composite mixture was used as working electrode. An E_S of ~52.6 Whkg⁻¹ with P_S of ~14000 Wkg⁻¹ is delivered by Co₃O₄+CuO based device which appear to be the best ever achieved in supercapacitor charge storage mode..

ABSTRAK

Kemunculan sektor tenaga boleh diperbaharui telah dikenalpasti, seiring dengan peranti pengubah tenaga dengan cekap, bahan elektrokimia yang mampu menyimpan tenaga elektrik pada kuantiti yang besar dan dapat digunakan pada kadar yang tinggi. Kapasitor elektrokimia merupakan suatu kelas peranti penyimpanan tenaga; kunci untuk mencapai ketumpatan tenaga (E_S) dan ketumpatan kuasa (P_S) yang tinggi ialah dengan mengoptimumkan keupayaan elektrod kerja. Bagaimanapun, E_S dan P_S tidak dapat dihubungkan pada peranti sediaada. Kebolehbalian elektrokimia yang tinggi, keadaan pengoksidaan yang pelbagai, luas permukaan tinggi dan konduktiviti elektrik yang tinggi merupakan keperluan untuk E_S dan P_S yang tinggi dalam elektrod superkapasitor. Kebanyakan bahan yang mempunyai kapasiti teori yang tinggi kesan dari kepelbagaian keadaan pengoksidaan mempunyai konduktiviti elektrik yang rendah; oleh yang demikian, hipotesis adalah konduktiviti elektrik memainkan peranan penting dalam menghubungkan E_S dan P_S di dalam peranti tunggal. Wayar-nano satu dimensi (1D) menunjukkan ciri penghantaran cas yang lebih baik berbanding analog partikel nano; oleh itu, struktur 1D dijangka memberikan E_S dan P_S secara serentak dengan baik dalam peranti tunggal. Kajian menunjukkan bahawa elektrod daripada bahan seramik menunjukkan kepelbagaian julat kapasiti dan konduktiviti berbanding bahan-bahan lain; oleh itu peranti sasaran dapat dihasilkan menggunakan elektrod seramik. Tiga bahan dengan morfologi wayar-nano telah dipilih bagi tujuan kajian ini, iaitu kuprum oksida (CuO), nikel oksida (NiO) dan kobalt oksida (Co₃O₄). Diantara bahan ini, secara teorinya, NiO dan Co₃O₄ mempunyai kapasiti masing-masing 2570 dan 3560 Fg⁻¹ berbanding CuO (1800 Fg⁻¹), dengan konduktiviti elektrik CuO lebih besar berbanding bahan lain. Penyediaan komposit merupakan salah satu kaedah untuk menggabungkan fungsi bahan berlainan; oleh itu, komposit CuO+NiO dan CuO+Co₃O₄ merupakan sasaran kajian. Bahan ini disintesis dalam bentuk wayar-nano 1D menggunakan larutan polimer cecair dengan proses electrospinning dan kajian dilakukan terhadap sifat-sifat struktur bahan menggunakan sinar-X dan pembelauan elektron, mikroskop transmisi elektron beresolusi tinggi; sifat-sifat morfologi menggunakan mikroskop imbasan elektron dan mikroskopi transmisi elektron; dan sifat-sifat elektrokimia menggunakan voltametri kitaran, kitaran cas-nyahcas dan spektroskopi impedan elektrokimia. Kajian elektrokimia menunjukkan bahawa CuO, NiO dan Co₃O₄ boleh mencapai kapasiti spesifik (C_S) menghampiri 30% daripada nilai teori, tetapi hanya pada kadar keupayaan rendah. Kajian menunjukkan komposit CuO+NiO dan CuO+Co₃O₄ mempunyai kadar keupayaan yang tinggi, rintangan sesiri dan rintangan pemindahan cas lebih rendah berbanding komponen tunggalnya. Superkapasitor tidak simetri (ASC) menggunakan anod seramik wayar-nano dan katod karbon teraktif komersil telah dihasilkan dan dibandingkan dari segi prestasi simpanan cas dengan superkapasitor simetri yang dihasilkan dengan hanya karbon teraktif pada kedua-dua elektrod. ASC menunjukkan C_S dan E_S dengan nilai tujuh kali lebih tinggi berbanding peranti simetri. P_S menurun dengan E_S yang dicapai untuk peranti yang menggunakan komponen seramik wayar-nano tunggal. Walau bagaimanapun, E_S tidak menunjukkan perubahan ketara dengan peningkatan P_S apabila komposit digunakan sebagai elektrod kerja. Peranti berasaskan CuO+Co₃O₄ menjana $E_S \sim 52.6 \text{ Whkg}^{-1}$ pada $P_S \sim 14000 \text{ Wkg}^{-1}$ menjadikan ia yang terbaik pernah dicapai bagi superkapasitor dalam mod simpanan cas.

TABLE OF CONTENTS

SUPERVISOR'S DECLARATION	iii
STUDENT'S DECLARATION	iv
ACKNOWLEDGEMENTS	vi
ABSTRACT	vii
ABSTRAK	viii
TABLE OF CONTENTS	ix
LIST OF TABLES	xiv
LIST OF FIGURES	xv
LIST OF SYMBOLS	xviii
ABBREVIATIONS	xix

CHAPTER I GENERAL INTRODUCTION

1.1 Introduction	1
1.2. Problem Statement	3
1.3 Objectives	4
1.4 Scope of the Thesis	5
1.5 Statement of Contribution	6
1.6 Organization of the Thesis	7

CHAPTER II	LITERATURE REVIEW	
2.1	Introduction	8
2.2	Electrical Double Layer Capacitors	9
2.3	Electrode Materials for EDLCs	10
2.3.1	Carbon Materials	11
2.3.2	Activated Carbon (AC)	11
2.3.3	Carbon Nanotube	12
2.3.4	Graphene	12
2.4	Pseudocapacitors	13
2.4.1	Pseudocapacitors with Under Potential Deposition	14
2.4.2	Pseudocapacitance with Redox Reaction	15
2.4.3	Pseudocapacitance with Doping and Dedoping	16
2.5	Material for Pseudocapacitor Electrodes	17
2.5.1	Conducting Polymers (CP)	17
2.5.1.1	Polyaniline	17
2.5.1.2	Polypyrrole	18
2.5.1.3	Other Polymers	18
2.5.2	Ceramics	18
2.5.2.1	$\text{RuO}_2 / \text{RuO}_{2 \cdot x}\text{H}_2\text{O}$	20
2.5.2.2	$\text{MnO}_2 / \text{MnO}_2$	23
2.5.2.3	$\text{Co}_3\text{O}_4 / \text{Co}_2(\text{OH})_4$	26
2.5.2.4	$\text{NiO} / \text{Ni}(\text{OH})_2$	29

2.5.2.5 CuO	31
2.6 Conclusions	33
CHAPTER III	MATERIALS AND METHODS
3.1 Research Methodology	36
3.2 Electrospinning Technique	38
3.3 Characterization	39
3.3.1 Powder X-ray Diffraction Technique	39
3.3.2 Thermogravimetric Analysis (TGA)	41
3.3.3 The Transmission Electron Microscope (TEM)	43
3.3.4 The Scanning Electron Microscope (SEM)	44
3.3.5 Energy Dispersive X ray Spectroscopy (EDS)	46
3.3.6 Brunauer–Emmett–Teller (BET) Measurement	46
3.3.7 Electrochemical Characterization	47
3.3.7.1 Cyclic Voltammetry	47
3.3.7.2 Chronopotentiometry	49
3.3.7.3 Electrochemical Impedance Spectroscopy (EIS)	49
3.4 Conclusions	50
CHAPTER IV	SYNTHESIS AND CHARACTERIZATION OF CERAMIC NANOWIRES BY ELECTROSPINNING TECHNIQUE
4.1 Introduction	51
4.2 Optimization of Polymeric Nanofibers	52

4.3 Morphology of Annealed Ceramic Nanowires	55
4.4 Crystal Structure of Ceramic Nanowires	61
4.4.1 CuO	61
4.4.2 NiO	64
4.4.3 Co ₃ O ₄	67
4.4.4. NiO+CuO composite	69
4.4.5 Co ₃ O ₄ +CuO composite	70
4.5 Surface Area and Pore Distribution Analysis	72
4.6 Conclusions	73

CHAPTER V ELECTROCHEMICAL PROPERTIES OF THE CERAMIC NANOWIRE ELECTRODES

5.1 Introduction	74
5.2. Preparation of Electrodes for Electrochemical Studies	74
5.3. Electrochemical Properties of Nanowires	75
5.3.1 Cyclic Voltammetry Studies	75
5.3.2 Galvanostatic Charge – Discharge Studies	87
5.3.3. Electrochemical Impedence Spectroscopy Studies	97
5.4 Electrochemical Characterization of Commercial Activated Aarbon	101
5.5 Conclusions	103

**CHAPTER VI FABRICATION AND TESTING OF ASYMMETRIC
SUPERCAPACITORS USING CERAMIC NANOWIRES AND
COMMERCIAL ACTIVATED CARBON**

6.1 Introduction	104	
6.2 Preparation of the Device	105	
6.3. Electrochemical Characterization	107	
6.3.1 Cyclic Voltammetry Studies	107	
6.3.2 Galvanostatic Charge – Discharge Studies	109	
6.3.3 Electrochemical Impedance Spectroscopy Studies	112	
6.4 Conclusions	119	
CHAPTER VII	SUMMARY AND RECOMMENDATIONS	120
REFERENCES		124
ACHIEVEMENTS		146

LIST OF TABLES

Table No	Title	Page
1.1	Capacitance, oxidation states, and electrical conductivities of six representative supercapacitor electrode materials	4
2.1	Summary of research on the use of RuO ₂ nanostructures and their composites with carbon structures/metal for application as a supercapacitor electrode	21
2.2	Summary of research on the use of MnO ₂ nanostructures and their composites with carbon structures/metals for application as a supercapacitor electrode	24
2.3	Summary of research on the use of Co ₃ O ₄ nanostructures and their composites with carbon structures/metals for application as a supercapacitor electrode	28
2.4	Summary of research on the use of NiO nanostructures and their composites with carbon structures/metals for application as a supercapacitor electrode	29
2.5	Summary of research on the use of CuO nanostructures and their composites with carbon structures/metals for application as a supercapacitor electrode	32
4.1	Comparison between previous and present protocol	53
4.2	A summary of the optimized electrospinning method used in this method	53
4.3	Summary of diameter and particle size of nanowire	61
4.4	Compared values of d spacing obtained from XRD and SAED of CuO	64
4.5	Compared values of d spacing obtained from XRD and SAED of NiO	66
4.6	Compared values of d spacing obtained from XRD and SAED of Co ₃ O ₄	68
4.7	Lattice parameters of materials obtained from XRD	72
4.8	The specific surface area, total pore volume and mean pore size of all materials	73
5.1	Summary of redox potentials and Coulombic efficiency observed from CV. R - Reversibility, η - Coulombic efficiency	77
5.2	Summary of internal resistance and C _S calculated from discharge curves	89
5.3	Summary of R _s , R _{ct} , f _o , and τ observed from EIS	100
6.1	Optimized mass ratio of electrodes	106
6.2	Summary of R _s and R _{ct} observed from Nyquist plot	113
6.3	Summary of research on the use of carbon nanostructures for application as a symmetric supercapacitor	116
6.4	Summary of research on the use of AC and different ceramic nanostructures for the fabrication of ASC	117

LIST OF FIGURES

Figure No.	Title	Page
1.1	Ragone plot for various energy storage devices	2
2.1	Representation of basic operation of a two electrode supercapacitor	8
2.2	The EDL structure based on Stern–Gouy Chapman model	9
2.3	Schematic of relation between charge stored/discharged and potential window during charge storage process of a supercapacitor and a lithium –ion battery for similar charge and discharge duration	13
2.4	Current vs. Potential relation for a pseudocapacitor with under potential deposition.	15
2.5	Charge storage mechanism in Conducting polymers	16
2.6	(a) Bar graph which shows the theoretical and practically achieved C_s of some of the widely used ceramics. (b)graph showing the rate capability of the ceramics;	34
2.7	Graph showing electrical conductivity of selected ceramic	34
3.1	Summary of methodology adopted in this work.	37
3.2	Schematic showing electrospinning set up	38
3.3	Photograph of electrospinning machine; Electroris	39
3.4	Schematics of lattice plane and diffraction of X-rays	40
3.5	Schematic of Thermal gravimetric analyser	42
3.6	Phograph of Thermal gravimetric analyser	42
3.7	(a) Photograph (b) Schematic view of Transmission Electron Microscope	44
3.8	(a) Photograph (b) Schematic of scanning electron microscope	45
3.9	Photograph and schematics of BET analyser	47
3.10	Photograph of Auto Lab PGSTAT M 101	48
3.11	(a) CV of a EDLC (b) CV of a pseudocapacitor	49
4.1	FESEM images of as prepared nanowires with different magnification	54
4.2	TGA curve of the as prepared composite wire	55
4.3	(a&b) FESEM images and (c&d)Bright field TEM images of CuO nanowires with different magnification	56
4.4	(a&b) FESEM images and (c&d) Bright field TEM images of NiO nanowires with different magnification	57
4.5	(a&b) FESEM images and (c&d) Bright field TEM images of Co_3O_4 nanowires with different magnification	58
4.6	(a&b) FESEM images and (c&d) Bright field TEM images of NiO+CuO nanowires with different magnification	59
4.7	(a&b) FESEM images and (c&d) Bright field TEM images of Co_3O_4 +CuO nanowires with different magnification	60
4.8	XRD pattern of copper oxide nanowire	62

4.9	TEM images of CuO nanowires; (a) selected area diffraction pattern (SAED), (b,c&d) high resolution lattice image of a typical particle in the TEM sample	63
4.10	XRD pattern of nickel oxide nanowire	65
4.11	TEM images NiO nanowires; (a) selected area electron diffraction, (b, c&d) high resolution lattice image of a typical particle in the TEM sample	66
4.12	XRD pattern of cobalt oxide nanowire	67
4.13	TEM images of Co ₃ O ₄ nanowires; (a) selected area diffraction pattern of a typical nanowire segment, (b,c&d) high resolution lattice image of a typical particle in the TEM sample	68
4.14	XRD pattern of (a) NiO+CuO composite nanowire (b) composite and its components.	69
4.15	TEM images of NiO+CuO nanowires (a) selected area electron diffraction image, (b) high resolution lattice image of a typical particle in the TEM image	70
4.16	XRD pattern of (a) Co ₃ O ₄ +CuO composite nanowire (b) composite and its components.	70
4.17	TEM images of Co ₃ O ₄ +CuO nanowires(a) FFT pattern corresponding HRTEM, (b,c &d) high resolution lattice image of a typical particle in the TEM image	71
5.1	Cyclic Voltammograms at 2 mVs ⁻¹ ; (a) CuO, (b) NiO, (c) Co ₃ O ₄ , (d) NiO+CuO, (e) Co ₃ O ₄ +CuO. A's and C's indicate oxidation and reduction events	76
5.2	CV curves at a scan rate 2 mVs ⁻¹ of CuO+ Co ₃ O ₄ composite at different mol. ratio; inset shows the variation of Cs with mol ratio	81
5.3	Cyclic Voltammograms of samples at different scan rate (a) CuO, (b) NiO, (c) Co ₃ O ₄ , (d) NiO+CuO (e) Co ₃ O ₄ +CuO	82
5.4	Variation of specific capacitance as a function of scan rate of all samples	83
5.5	Anodic peak current as a function of square root of scan rate; (a) CuO, (b) NiO, (c) Co ₃ O ₄ , (d) NiO+CuO composites, (e) Co ₃ O ₄ +CuO composites	84
5.6	Anodic peak current as a function of (a) scan rate of the CuO electrode in 3M KOH and (b) the square root of scan rate in 3M LiOH	85
5.7	Fraction of active sites involved in the electrochemical reaction calculated using CV data	86
5.8	First three charge discharge curves; (a) CuO, (b) NiO, (c) Co ₃ O ₄ , (d) NiO+CuO, (e) Co ₃ O ₄ +CuO	88
5.9	Discharge curves at 1 Ag ⁻¹ of CuO+Co ₃ O ₄ composite wire at different mol. ratio. Insets shows the variation of Cs with mol. ratio	90
5.10	Discharge curves at different current densities; (a) CuO, (b) NiO, (c) Co ₃ O ₄ , (d) NiO+CuO, (e) Co ₃ O ₄ +CuO	92

5.11	Variation of specific capacitance as a function of current density of all samples	93
5.12	Dependence of the discharge specific capacitance and the Coulombic efficiency as a function of charge discharge cycle	94
5.13	Dependence of discharge specific capacitance as a function of charge discharge cycle numbers at progressively varying current densities (a) NiO+CuO (b) Co ₃ O ₄ +CuO	96
5.14	Nyquist plot of samples at open circuit potential; inset: a magnified high frequency region of the spectrum showing the equivalent series resistance of the electrode; (a) CuO, (b) NiO, (c) Co ₃ O ₄ , (d) NiO+CuO, and (e) Co ₃ O ₄ +CuO	98
5.15	The variation of the real (C') and imaginary (C'') part of capacitance with frequency at open circuit potential for (a) CuO, (b) NiO, (c) Co ₃ O ₄ , (d) NiO+CuO, (e) Co ₃ O ₄ +CuO	100
5.16	a) Cyclic voltammograms of AC at different scan rate(b) variation of Cs with scan rate(c) two charge discharge curve(d) discharge curves at various current density(e) variation of Cs with current density (f) Nyquist plot at open circuit potential	102
6.1	Schematic diagram of a ASC fabricated using ceramic nanowire and activated carbon	105
6.2	Cyclic voltammograms (a) AC//AC, (b) CuO//AC, (c) Co ₃ O ₄ //AC, (d) Co ₃ O ₄ +CuO//AC	107
6.3	Variation of Specific capacitance as a function of scan rate	108
6.4	First three charge discharge curves (a) AC//AC (b) CuO//AC (c) Co ₃ O ₄ //AC (d) Co ₃ O ₄ +CuO//AC	109
6.5	Discharge curves at different current densities (a) AC//AC (b) CuO//AC (c) Co ₃ O ₄ //AC (d) Co ₃ O ₄ +CuO//AC	110
6.6	Variation of Specific capacitance with current density	111
6.7	Dependence of the discharge specific capacitance and the Coulombic efficiency as a function of charge discharge cycle	111
6.8	Dependence of discharge specific capacitance as a function of charge discharge cycle numbers at progressively varying current densities	112
6.9	Nyquist plot of samples at open circuit potential	113
6.10	A magnified high frequency region of the Nyquist plot showing the equivalent series resistance (ESR) of the device	114
6.11	Comparative Ragone plots of the symmetric and asymmetric supercapacitors	115

LIST OF SIMBOLS

ω	Angular frequency
ε	Permittivity of the medium
σ	Ionic conductivity
γ	Gamma
β	Beta
δ	Delta
α	Alpha
θ	Angle
ρ	Density
τ	Relaxation time
π	Pi

ABBREVIATIONS

AC	- Activated carbon
ASC	- Asymmetric supercapacitor
BET	- Brunauer Emmett Teller
CNT	- Carbon nanotube
1D	- One dimensional
EDLC	- Electrical double layer capacitor
ESR	-Equivalent series resistance
FFT	- Fast Fourier Transform
GO	- Graphene oxide
IHP	- Inner Helmholtz plane
MPC	- Mesoporous carbon
OHP	- Outer Helmholtz plane
PC	- Pseudocapacitor
RGO	- Reduced graphene oxide
SAED	- Selected area electron diffraction
SWCNT	- Single wall carbon nanotube
TGA	- Thermal gravimetric analysis
TEM	- Transmission electron microscopy
XRD	- X- ray diffraction
Fg ⁻¹	- Farad per gram
mVs ⁻¹	- milli Volt per second
Ag ⁻¹	- Ampere per gram
kWkg ⁻¹	- kilowatt per kilogram
Whkg ⁻¹	- Watt hour per kilogram
nm	- nanometre
cP	- centipoise
NR	- Not reported

CHAPTER I

GENERAL INTRODUCTION

1.1 INTRODUCTION

Energy production and dissemination determine the quality of human life in modern society: large energy expenditure is required to have a high quality life. Increase in human population and flourishing of more energy intensive equipment lead in a rapid increase in the energy demand. On the other hand, depletion of natural sources such as fossil fuels necessitates harnessing energy from sustainable sources such as sun, wind, and water. In order for the sustainable sources to become completely dependable as primary sources of energy, energy storage devices are highlighted as essential components in addition to efficient energy conversion devices (Dell and Rand, 2001; Rand, 2011). Batteries, capacitors and supercapacitors are preliminary energy storage devices with differing storage capabilities rationalized in terms of energy and power densities. Energy density is the amount of electrical energy that can be stored and power density is the rate at which the energy is stored/delivered. The Ragone plot, which relates specific energy (E_S) and power densities (P_S), of popular energy storage devices projected for the 21st century is in Figure 1.1 (Rolison and Nazar, 2011). Batteries have high E_S ($>200 \text{ Whkg}^{-1}$) but have low P_S ($<500 \text{ Wkg}^{-1}$); therefore, they are the most widely used storage systems. On the other hand, conventional capacitors have high P_S ($\sim 10^7 \text{ Wkg}^{-1}$) but very low E_S ($<10^{-1} \text{ Whkg}^{-1}$). The performance of these two devices are short range of E_S and P_S ; a single device covers most of the energy spectrum is the electrochemical capacitors (ECs) or supercapacitors. The ECs offer potentially higher P_S ($>10^6 \text{ Wkg}^{-1}$) and higher E_S (1000 Whkg^{-1}); and therefore, they have emerged as one of the advanced energy storage system and find use in trucks,

portable tool kits, bus, airplanes as well as in heavy duty construction and railways in powering yard cranes and bullet trains (Rolison and Nazar, 2011).

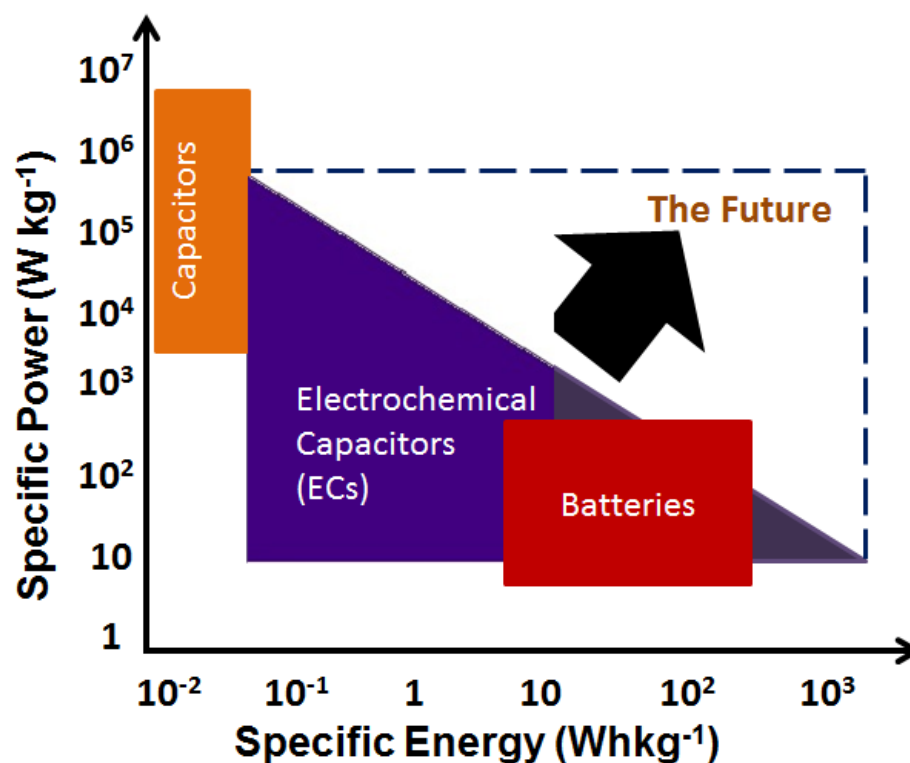


Figure 1.1: Ragone plot for various energy storage devices. Adapted with permission from (Rolison and Nazar, 2011).

The ECs are classified into electrochemical double layer capacitors (EDLCs), pseudocapacitors (PCs), and hybrid capacitors (HCs) based on the charge storage mechanism. The EDLC store electrical energy via accumulation of electric charges at an electrical double layer formed at the interface between a mesoporous electrode and an electrolyte. Carbon structures such as activated carbon, carbon nanotubes, and graphene are choices to build EDLCs. No electron transfer takes place across the electrode - electrolyte interface during its operation; and therefore, this charge storage process is non-faradic. The PCs involve faradic charge storage process facilitated by a redox reaction at the electrode – electrolyte interface. Transition metal oxides (TMOs), i.e., ceramics, and conducting polymers show high pseudocapacitance; a theoretical pseudocapacitance equal to $(n \times F) / (\Delta E \times m)$, where F is the Faraday constant, n number of electrons involved, m is the molecular weight and ΔE is the redox potential

of the material, could be achieved by ceramics. A high specific surface area of the electrode material to enable a large electrode – electrolyte interface for efficient redox reaction, high electrical conductivity to enable high rate charging and discharging, and faster ion diffusivity are properties of ceramics and electrolytes required to achieve higher E_S and P_S in PCs. The HCs combine both storage mechanisms, i.e., EDLC and PC, in a single material.

The ECs consist of two electrodes, a separator and an electrolyte and consequently two device configurations are proposed with varied choice of electrode operating mechanism, viz. symmetric and asymmetric supercapacitors (Conway, 1997; Ko, R. and Carlen, 2000). In a symmetric supercapacitor (SSCs), both electrodes operate under similar charge storage mechanism whereas one of the electrodes in asymmetric supercapacitors (ASCs) is EDLC and the other is PC.

1.2 PROBLEM STATEMENT

High electrochemical reversibility, multiple oxidation states, high surface area and high electrical conductivity are requirements for high P_S and E_S electrode materials for supercapacitors. Among these requirements, oxidation state and electrical conductivity are the intrinsic properties. To draw a relationship between oxidation state and electrical conductivity on the achievable capacitance of supercapacitor electrodes, consider six representative ceramics supercapacitor electrodes with varied oxidation states and electrical conductivity, viz. CuO, NiO, Co₃O₄, RuO₂, MnO₂, and V₂O₅. The theoretical capacitance, practically achieved capacitance, number of oxidation states and electrical conductivity of these materials are summarized in Table 1.1 based on a literature survey described in the next chapter. Although Co₃O₄ has multiple oxidation states its low electrical conductivity poses a challenge for achieving high practical capacitance. On the other hand CuO, NiO and RuO₂ achieved high capacitance because of high electrical conductivity. So it is hypothesised that composite of electrochemical materials having multiple oxidation states and high electrical conductivity is likely to generate an electrode material with high P_S and E_S . Furthermore, one-dimensional (1D) nanowires show improved charge transport properties compared to their nanoparticle analogue; therefore, 1D structures are expected to deliver simultaneously E_S and P_S .

Table 1.1: Capacitance, oxidation states, and electrical conductivities of six representative supercapacitor electrode materials

Ceramics/ Properties	Theoretical capacitance(Fg^{-1})	Practically achieved capacitance (Fg^{-1})	Number of redox state	Electrical conductivity (Scm^{-1})
CuO	1800	900	1	$10^{-2} - 10^{-3}$
NiO	2570	1800	1	$10^{-2} - 10^{-3}$
RuO ₂	1300	1200	1	10^2
Co ₃ O ₄	3560	1350	4	$10^{-3} - 10^{-4}$
MnO ₂	1360	700	4	$10^{-2} - 10^{-5}$
V ₂ O ₅	2200	400	4	$10^{-2} - 10^{-6}$

Among the many nanowire forming techniques, electrospinning represents a simple and versatile technique for producing nanostructured advanced materials as well as membranes for many engineering applications to be enabled such as filtration, healthcare, and energy (Ramakrishna et al., 2010; Reneker and Yarin, 2008; Sigmund et al., 2006). In the electrospinning technique, a polymeric solution, usually prepared in organic solvents, is injected through a syringe needle in the presence of an electric field. A polymeric jet is initiated upon injection of the solution that undergoes asymmetric bending during the passage between the injector and the collector. This asymmetric bending increases the path length of the jet and allows the solvent to evaporate thereby producing solid continuous fibers with diameters ranging from nanometers to sub-micrometers on a collector surface. If the polymeric solution contains precursors for forming an inorganic solid, then appropriate annealing produces its continuous nanofibers (Bhardwaj and Kundu, 2010). However, evaporation of large volume of organic solvents during electrospinning have adverse environmental effects; this drawback is removed in “greener” electrospinning using aqueous polymeric solutions.

1.3 OBJECTIVES

Ultimate goal of this thesis is to develop an EC that combine E_S and P_S in a single device and that can be commercially developed; therefore, preferred device configuration is an ASC. As universally one of the electrodes in ASC is EDLC, the problem reduces to the second electrode. The ceramic electrode materials, as will be

detailed in Chapter 2 of this thesis, show diverse range of capacitance and conductivities than conducting polymers and hybrid materials; therefore, the target device could be achieved using ceramic electrodes. Three typical materials with nanowire morphology are chosen for this purpose, viz. copper oxide (CuO), nickel oxide (NiO), and cobalt oxide (Co₃O₄). Among them NiO and Co₃O₄ show larger theoretical capacitance, 2570 and 3560 Fg⁻¹, respectively, than that of CuO (1800 Fg⁻¹) but has larger electrical conductivity than the other two. Synthesizing a composite is the simplest method to combine the functions of different materials; therefore, it is expected that CuO+NiO and Co₃O₄+CuO composites are the target materials. To achieve the final goal, the following research objectives are visualized.

1. To develop nanowires of CuO, NiO, Co₃O₄, NiO+CuO and Co₃O₄+CuO composites using an aqueous polymeric solution based electrospinning technique with desirable crystallinity and surface properties.
2. To evaluate the electrochemical properties and energy storage capabilities of the above ceramic nanowires in aqueous electrolytes of high conductivity.
3. To demonstrate the usefulness of the above materials for energy storage devices by fabricating ASCs using them as anode and commercial activated carbon as cathode and to evaluate their charge storage capabilities.

By achieving the objectives, the research undertaken could produce an electrochemical material, which is a nanowire composing the nanoparticles of CuO and Co₃O₄, that could support high energy and power densities with high degree of rate capabilities

1.4 SCOPE OF THE THESIS

The following research activities are required to achieve the first objective:

- i. Optimising the viscosity of the electrospinning polymer solutions for developing uniform nanowires. Evolution of the nanowire morphology could be examined using scanning electron microscopy.
- ii. To optimize electrospinning parameters such as, voltage between the needle and the collector, the distance between them to tailor the diameter of the ceramic nanowires.

- iii. To study the decomposition behaviour of the electrospun polymeric mat when it is heated to develop the ceramic nanowires by a thermogravimetric analysis.
- iv. Crystal structure, lattice parameter, spacing between plans and the grain size could be identified from XRD and TEM measurements. Crystal defects are identified from HRTEM images.

As for the second objective, following research activities are required to achieve it.

- i. Optimize the mass loading of active material, PVDF and conducting carbon in the preparation of the electrode for electrochemical evaluation.
- ii. Optimize the electrolyte and its concentration to obtain maximum capacitance and stability.
- iii. Study the charge discharge behaviour by cyclic voltammetry (CV) and galvanostatic charge discharge cycling (CDC) behaviour.
- iv. Study the variation of specific capacitance as functions of scan rate and current density employed during CV and CDC measurements.
- v. Determine the structure-property correlation between electrochemical property and structure of the material by Faraday's equation as well as dependence of voltammetric current on the scan rate.
- vi. Evaluate the electrochemical recyclability from CV and CDC experiments and calculate the Coulombic efficiency.
- vii. To study the electrode kinetics using electrochemical impedance spectroscopy (EIS).
- viii. To deduce electrode kinetic parameters using EIS

Finally for the third objectives following are the activities required to achieve it.

- i. Optimizing the mass of the active materials at the anode and cathode of symmetric and asymmetric supercapacitor device such that the ratio remains same for best performance.
- ii. Fabrication of a working supercapacitive device in proper device geometry and suitable for operation.
- iii. Characterization of the device to study the charge storage mechanism both in the symmetric and asymmetric device structures by cyclic voltammetry, charge –

discharge cycling, and electrochemical impedance spectroscopy under various experimental conditions of scan rate and current density.

- iv. Evaluation of the energy storage capabilities by drawing the Ragone plot.

1.5 STATEMENT OF CONTRIBUTION

Nanocomposite nanowires of two electrochemical materials, one with large specific capacitance and the other with high electrical conductivity, were synthesized for the first time. The nanowire nanocomposite thus developed united high P_S and E_S when they were used as anode for asymmetric supercapacitors. Asymmetric supercapacitors delivering E_S of $\sim 52.6 \text{ Whkg}^{-1}$ at P_S of $\sim 14 \text{ kWkg}^{-1}$ were realized for the first time based on these developments; a combination of such P_S and E_S has not been achieved before. Efforts are currently underway to develop viable market products.

1.6 ORGANIZATION OF THE THESIS

Starting from a brief introduction to ECs,

- Chapter 1: Presents problem statement, research objectives, scope and statement of contribution of research.
- Chapter 2: Reports a comprehensive review on the working principle of supercapacitor and varied choice of the electrode material used.
- Chapter 3: Presents the experimental method used in this work and the working principle of the instruments used for characterization.
- Chapter 4: Discusses the synthesis and characterization of CuO, NiO, Co_3O_4 , and NiO+CuO composite and Co_3O_4 +CuO composite.
- Chapter 5: Evaluate the result of electro-chemical studies of electrospun ceramic wires in aqueous electrolytes.
- Chapter 6: Illustrates the research work on the fabrication of asymmetric supercapacitor by ceramic nanowires and activated carbon and its electrochemical performance.
- Chapter 7: Gives the summary of this work and the recommendations for future work.

CHAPTER II

LITERATURE REVIEW

2.1 INTRODUCTION

This chapter provide a brief account of the structure and energy storage mechanism in electrochemical capacitors or also called supercapacitors. The chapter further evaluate the recent research progress achieved in the electrochemical performance in terms of specific capacitance (C_S), energy density (E_S), power density (P_S) and cycle life of electrode material used for supercapacitors.

As mentioned in the Chapter 1, ECs consist of two electrodes, a separator and an electrolyte as in Figure 2.1. As stated before, symmetric supercapacitors (SSCs) form when both of the electrodes are EDLC and ASCs when one of them is EDLC and the other is PC (Conway, 1997; Ko, R. and Carlen, 2000).

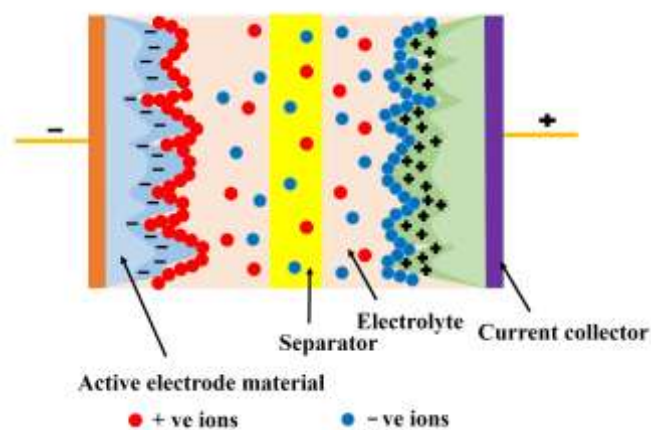


Figure 2.1: Representation of the basic operation of a two electrode supercapacitor

The EC electrodes are broadly classified into two based on their charge storage mechanism, viz. electric double layer capacitors (EDLC) and pseudocapacitors (PC) (Conway, 1997; Wang, G. et al., 2012; Zhang, J. and Zhao, 2012; Zhang, L. L. and Zhao, 2009). The following passage gives a brief description on the phenomenology and materials used in both types. The performance achieved by each type and materials also summarized.

2.2 ELECTRICAL DOUBLE LAYER CAPACITORS

When a solid electrode is placed in an electrolyte an electric double layer (EDL) is formed at the interface between the electrode and electrolyte. EDL is similar to an electric dipole and possess a potential; the EDLCs make use of this potential for storing electric charge. Several models, viz. Helmholtz model, Gouy- chapman model, and Grahame model have been proposed to explain the EDLCs. The Helmholtz model states that whenever a particular charge is accumulated on the electrode surfaces and ions of opposite charge are arranged on electrolyte side. Helmholtz model could not explain the variation of capacitance with surface potential or ion concentration. In 1910, Gouy and Chapman assumed a continuous distribution of electrolyte ions in the electrolyte solution, which is termed as the diffusive layer (Figure 2.2)(Conway, 1997).

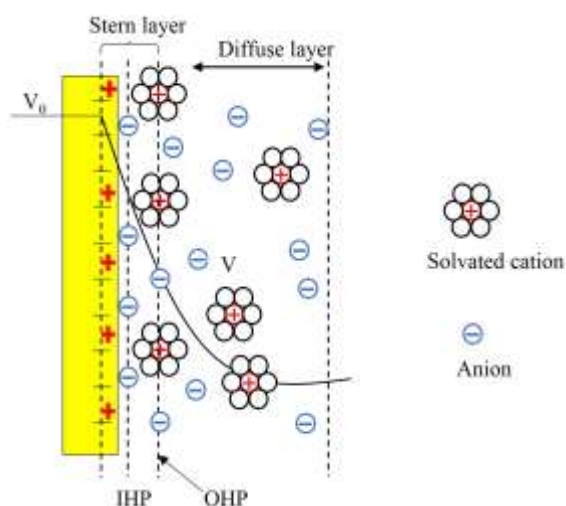


Figure 2.2: The EDL structure based on Stern –Gouy Chapman model. Adapted with permission from (Zhang, 2007).IHP-inner Helmholtz plane, OHP outer Helmholtz plane, V -potential

Later, Stern combined the Helmholtz model with the Gouy – Chapman model to explicitly recognize two regions of ion distribution – the inner region is called stern layer and outer layer is called the diffusive layer (Figure 2.2)(Conway, 1997).

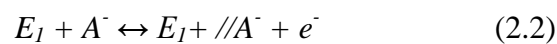
The Stern layer consist of specifically adsorbed ions called inner Helmholtz plane (IHP) and non-specifically adsorbed counter ions called outer Helmholtz plane (OHP).The IHP in the electrolyte was considered compact and the potential profile in the EDL decreased linearly with the distance from the electrode surface. The capacitance in the EDL (C_{dl}) can be considered as sum of capacitances from the stern type of compact double layer capacitance (C_H) and the diffusion region capacitance (C_{diff}). Then the net capacitance can be calculated using the equation:

$$\frac{1}{C_{dl}} = \frac{1}{C_H} + \frac{1}{C_{diff}} \quad (2.1)$$

There is no charge transfer between the electrode/electrolyte interface, and anions and cations in the electrolyte moved within the electrolyte to the charged surface. This is the reason why the charging and discharging processes of an EDLC are highly reversible.

The electrochemical processes for charging and discharging can be expressed as:

On the anode



On the Cathode



2.3 ELECTRODE MATERIALS FOR EDLCs

High surface area, uniform pore distribution, pore size and good electrical conductivity are the important features for the EDLC electrode materials. Further, the capacitance could be enhanced by suitably choosing electrolytes depending on the pore structure of the electrode material (Misono et al., 2014). i.e., the electrode show the maximum performance if the solvated ion size is similar to the pore size of the electrode. Carbon materials with high surface area and tailored pore distribution, such

CHAPTER I

GENERAL INTRODUCTION

1.1 INTRODUCTION

Energy production and dissemination determine the quality of human life in modern society: large energy expenditure is required to have a high quality life. Increase in human population and flourishing of more energy intensive equipment lead in a rapid increase in the energy demand. On the other hand, depletion of natural sources such as fossil fuels necessitates harnessing energy from sustainable sources such as sun, wind, and water. In order for the sustainable sources to become completely dependable as primary sources of energy, energy storage devices are highlighted as essential components in addition to efficient energy conversion devices (Dell and Rand, 2001; Rand, 2011). Batteries, capacitors and supercapacitors are preliminary energy storage devices with differing storage capabilities rationalized in terms of energy and power densities. Energy density is the amount of electrical energy that can be stored and power density is the rate at which the energy is stored/delivered. The Ragone plot, which relates specific energy (E_S) and power densities (P_S), of popular energy storage devices projected for the 21st century is in Figure 1.1 (Rolison and Nazar, 2011). Batteries have high E_S ($>200 \text{ Whkg}^{-1}$) but have low P_S ($<500 \text{ Wkg}^{-1}$); therefore, they are the most widely used storage systems. On the other hand, conventional capacitors have high P_S ($\sim 10^7 \text{ Wkg}^{-1}$) but very low E_S ($<10^{-1} \text{ Whkg}^{-1}$). The performance of these two devices are short range of E_S and P_S ; a single device covers most of the energy spectrum is the electrochemical capacitors (ECs) or supercapacitors. The ECs offer potentially higher P_S ($>10^6 \text{ Wkg}^{-1}$) and higher E_S (1000 Whkg^{-1}); and therefore, they have emerged as one of the advanced energy storage system and find use in trucks,

portable tool kits, bus, airplanes as well as in heavy duty construction and railways in powering yard cranes and bullet trains (Rolison and Nazar, 2011).

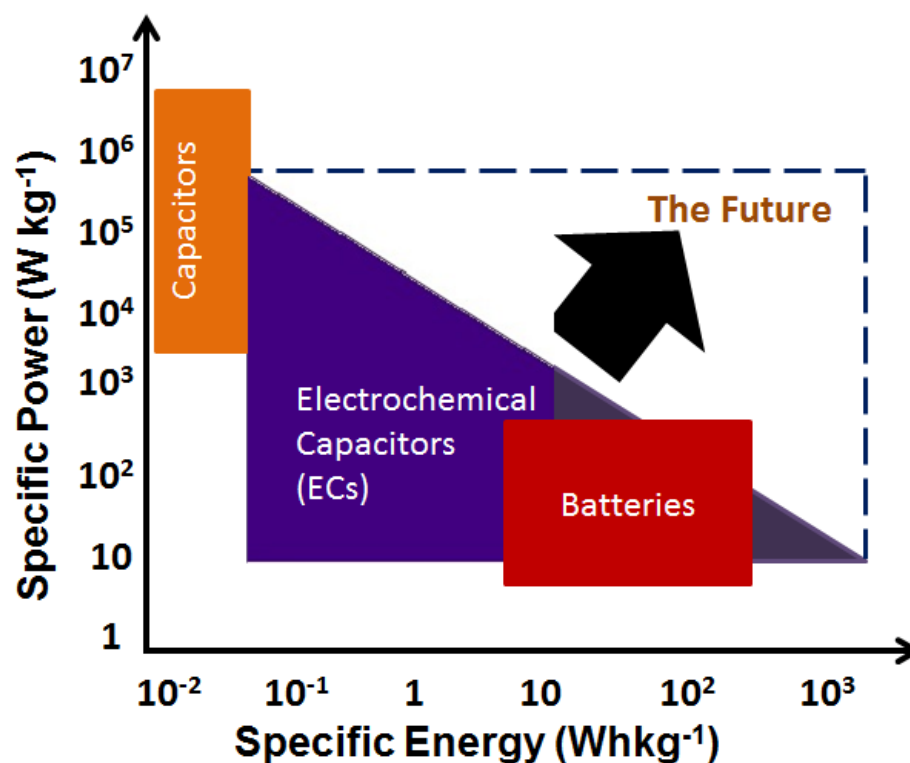


Figure 1.1: Ragone plot for various energy storage devices. Adapted with permission from (Rolison and Nazar, 2011).

The ECs are classified into electrochemical double layer capacitors (EDLCs), pseudocapacitors (PCs), and hybrid capacitors (HCs) based on the charge storage mechanism. The EDLC store electrical energy via accumulation of electric charges at an electrical double layer formed at the interface between a mesoporous electrode and an electrolyte. Carbon structures such as activated carbon, carbon nanotubes, and graphene are choices to build EDLCs. No electron transfer takes place across the electrode - electrolyte interface during its operation; and therefore, this charge storage process is non-faradic. The PCs involve faradic charge storage process facilitated by a redox reaction at the electrode – electrolyte interface. Transition metal oxides (TMOs), i.e., ceramics, and conducting polymers show high pseudocapacitance; a theoretical pseudocapacitance equal to $(n \times F) / (\Delta E \times m)$, where F is the Faraday constant, n number of electrons involved, m is the molecular weight and ΔE is the redox potential

of the material, could be achieved by ceramics. A high specific surface area of the electrode material to enable a large electrode – electrolyte interface for efficient redox reaction, high electrical conductivity to enable high rate charging and discharging, and faster ion diffusivity are properties of ceramics and electrolytes required to achieve higher E_S and P_S in PCs. The HCs combine both storage mechanisms, i.e., EDLC and PC, in a single material.

The ECs consist of two electrodes, a separator and an electrolyte and consequently two device configurations are proposed with varied choice of electrode operating mechanism, viz. symmetric and asymmetric supercapacitors (Conway, 1997; Ko, R. and Carlen, 2000). In a symmetric supercapacitor (SSCs), both electrodes operate under similar charge storage mechanism whereas one of the electrodes in asymmetric supercapacitors (ASCs) is EDLC and the other is PC.

1.2 PROBLEM STATEMENT

High electrochemical reversibility, multiple oxidation states, high surface area and high electrical conductivity are requirements for high P_S and E_S electrode materials for supercapacitors. Among these requirements, oxidation state and electrical conductivity are the intrinsic properties. To draw a relationship between oxidation state and electrical conductivity on the achievable capacitance of supercapacitor electrodes, consider six representative ceramics supercapacitor electrodes with varied oxidation states and electrical conductivity, viz. CuO, NiO, Co₃O₄, RuO₂, MnO₂, and V₂O₅. The theoretical capacitance, practically achieved capacitance, number of oxidation states and electrical conductivity of these materials are summarized in Table 1.1 based on a literature survey described in the next chapter. Although Co₃O₄ has multiple oxidation states its low electrical conductivity poses a challenge for achieving high practical capacitance. On the other hand CuO, NiO and RuO₂ achieved high capacitance because of high electrical conductivity. So it is hypothesised that composite of electrochemical materials having multiple oxidation states and high electrical conductivity is likely to generate an electrode material with high P_S and E_S . Furthermore, one-dimensional (1D) nanowires show improved charge transport properties compared to their nanoparticle analogue; therefore, 1D structures are expected to deliver simultaneously E_S and P_S .

CHAPTER III

MATERIALS AND METHODS

3.1 INTRODUCTION

This chapter details the research methodology which comprises of various materials and methods used in the present research. The details of the synthesis protocol and development of nanowires, the tools and techniques used for characterizations of the materials, the possible errors, the precautions and correction made, preparation and testing of supercapacitor electrodes, and fabrication of asymmetric supercapacitors and testing is elaborated in this chapter.

3.2 RESEARCH METHODOLOGY

Flowchart 3.1 outlines the research methodology adopted in this work. The materials were synthesized by electrospinning technique using an aqueous polymeric solution based electrospinning; the as-spun polymeric fibers were annealed to get ceramic nanowires; the nanowires thus obtained were characterized for its morphology, crystal structure, and surface properties. The supercapacitor electrodes were fabricated using those nanowires and tested their electrochemical properties. Finally asymmetric supercapacitors were fabricated using the nanowires as one of the electrodes and commercial activated carbon as the other electrode; the devices were tested electrochemically. The techniques used for synthesis, characterization, device fabrication, and testing are detailed in this chapter subsequently.

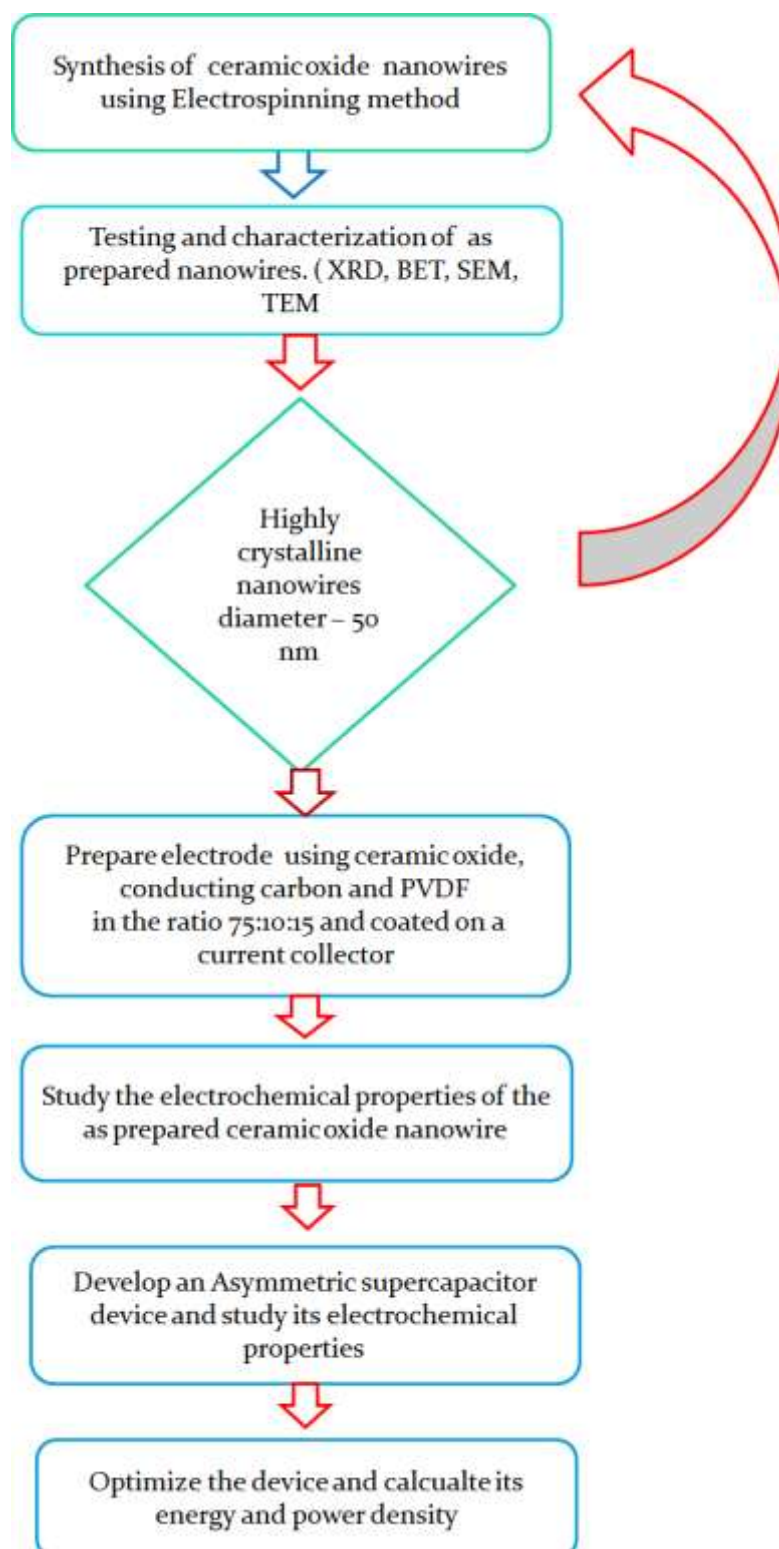


Figure 3.1: Summary of methodology adopted in this work.

3.2 ELECTROSPINNING TECHNIQUE

The electrospinning is a simple technique for fabrication of continuous nanofibers of polymers and polymeric composites (Ramakrishna et al., 2010; Reneker and Yarin, 2008). A typical electrospinning set up consists of a high voltage power supply, a programmable syringe pump and a grounded collector as in Figure 3.2&3.3. During the process, a polymeric solution is injected from a small nozzle in a region of high electric field ($\sim 10^5 \text{Vm}^{-1}$). The build-up of electrostatic charge on the surface of a liquid droplet induces the formation of a jet, which is then stretched to form a continuous fibre. The solution evaporates before it reaches the collecting drum and solid fibers are collected.

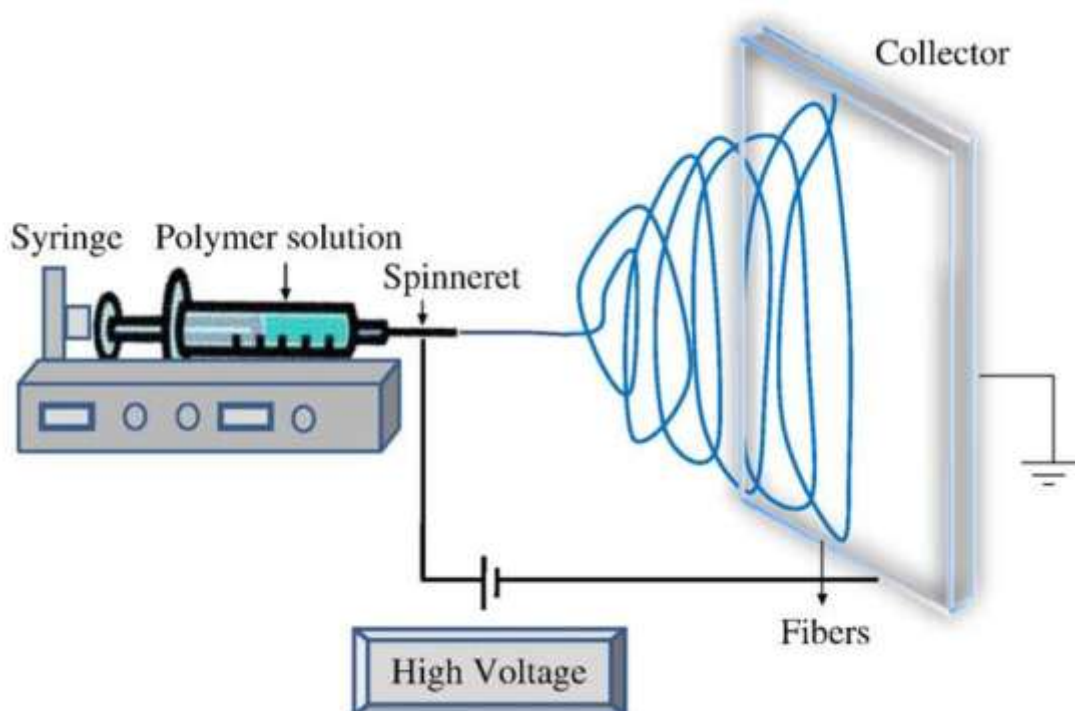


Figure 3.2: Schematic showing electrospinning set up. Adapted from (Bhardwaj and Kundu, 2010).

The electrospinning process is controlled by three parameters, viz. (i) solution parameters, (ii) process parameters, and (iii) ambient parameters. The solution parameters include viscosity, conductivity, molecular weight, and surface tension (Bhardwaj and Kundu, 2010). The process parameters include applied electric field, needle to collector distance, and flow rate. The ambient parameters include humidity